The University Of Sheffield.

This is a repository copy of *Tri-band single chain radio receiver for concurrent radio*.

White Rose Research Online URL for this paper:
https://eprints.whiterose.ac.uk/187413/

Version: Accepted Version

Proceedings Paper:
Henthorn, S. orcid.org/0000-0003-1913-9283, O'Farrell, T. orcid.org/0000-0002-7870-4097, Asif, S.M. et al. (2 more authors) (2020) Tri-band single chain radio receiver for concurrent radio. In: 2020 2nd 6G Wireless Summit (6G SUMMIT). 2020 2nd 6G Wireless Summit (6G SUMMIT), 17-20 Mar 2020, Levi, Finland. Institute of Electrical and Electronics Engineers . ISBN 9781728160481

https://doi.org/10.1109/6GSUMMIT49458.2020.9083776

© 2020 IEEE. Personal use of this material is permitted. Permission from IEEE must be obtained for all other users, including reprinting/ republishing this material for advertising or promotional purposes, creating new collective works for resale or redistribution to servers or lists, or reuse of any copyrighted components of this work in other works. Reproduced in accordance with the publisher's self-archiving policy.

Reuse
Items deposited in White Rose Research Online are protected by copyright, with all rights reserved unless indicated otherwise. They may be downloaded and/or printed for private study, or other acts as permitted by national copyright laws. The publisher or other rights holders may allow further reproduction and re-use of the full text version. This is indicated by the licence information on the White Rose Research Online record for the item.

Takedown
If you consider content in White Rose Research Online to be in breach of UK law, please notify us by emailing eprints@whiterose.ac.uk including the URL of the record and the reason for the withdrawal request.

White Rose university consortium
Universities of Leeds, Sheffield & York

eprints@whiterose.ac.uk
https://eprints.whiterose.ac.uk/

Tri-band Single Chain Radio Receiver for Concurrent Radio

S. Henthorn, T. O'Farrell, S.M. Asif, M.R. Anbiyaei, K.L. Ford
Department of Electronic and Electrical Engineering
University of Sheffield
Sheffield, UK
t.ofarrell@sheffield.ac.uk

***Abstract*— The bandwidth available for improving throughputs to future mobile devices at sub-6 GHz frequencies can be increased through aggregating multiple non-contiguous bands, which may be using the same or different radio access technologies to transmit information. However, with conventional radio technology, a complete radio frequency (RF) chain is required for each band, limiting the possible increase due to space and energy consumption restraints in the mobile station (MS). This paper presents and measures a single RF chain radio for concurrent reception of three non-contiguous bands transmitting 16-QAM LTE signals, using a tunable analogue front-end and software defined radio (SDR) techniques. The receiver sensitivity is degraded by only 6dB under worst-case concurrent reception, compared with reception of a single band. This demonstrates that complex signaling techniques can be received concurrently with a single radio chain while meeting the 3GPP standards, opening the way to compact, efficient, multiband receivers for future standards.**

Keywords—Software defined radio; direct RF digitisation; common sampling frequency; multiband radios; tunable antennas; beyond 5G.

I. INTRODUCTION

As with previous generations of mobile communications networks, the change from 5G systems to 6G is being driven by the need to increase both total capacity and throughput to individual devices [1]. One of the key ways this will be achieved is through using greater signal bandwidths, both by moving to higher carrier frequencies where more contiguous spectrum is available [2], and through carrier aggregation (CA) between multiple bands at lower frequencies [3]. This latter case is particularly of interest in emerging heterogeneous network (HetNet) architectures in 5G and beyond [4].

However, using conventional radio technology, separate receivers are required for different bands, largely due to the limitations of the radio frequency (RF) front-end [5]. This causes particular problems at the mobile station (MS) handset, which has limited space and power consumption. As such, inter-band CA is currently utilized in only limited situations. Further, even where emerging technologies such as software defined radio (SDR) methods are used, only a single standard can be processed by the radio at a time. This limits the potential for total throughput to be increased by using both contemporary and legacy standards.

This paper presents a receiver architecture that allows concurrent multiband processing of up to three different RF bands, using a single RF chain. The receiver utilizes direct digitization of all bands using a common sampling frequency, followed by digital down-conversion of each band to recover the baseband signals. This is enabled by an RF front-end consisting of a tunable, triband slot antenna; a broadband low noise amplifier (LNA) with high dynamic range; a bank of surface acoustic wave (SAW) filters; and post-amplification of the filtered signals. All bands examined are below 6 GHz, for extensive coverage. For demonstration, LTE signals carrying 16-QAM modulated data are transmitted and received in each band, though different standards could be used. The performance of the system is evaluated through the constellation error vector magnitude (EVM) and the system block error rate (BLER). The results show that a receiver with a single RF chain can be designed, which is capable of supporting concurrent multi-band reception of complex, higher-order signals with acceptable sensitivity.

II. CONCURRENT, MULTIBAND RECEIVER ARCHITECTURE

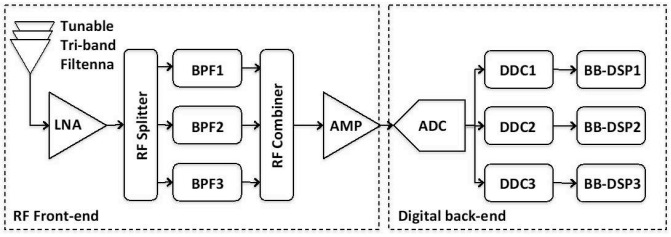

Fig. 1. Tunable, concurrent, tri-band receiver architecture.

The single-chain concurrent multiband receiver architecture, shown in Fig. 1, consists of two main sections: a RF front-end, consisting of a tunable tri-band antenna, amplifiers and filtering; and a digital back-end, where analog-to-digital conversion (ADC) of the whole RF domain is performed, and then each band is separately downconverted using a digital downconverter (DDC), and the baseband (BB) signals processed to retrieve the transmitted data. This process of placing the ADC as close to the antenna as possible, so removing the need for separate downconverters for each band,

makes the receiver more compact and flexible, in common with SDR approaches [6]. The three bands explored in this paper are 888 MHz, 1.92 GHz and 2.53 GHz. The two parts of the receiver are now examined in detail.

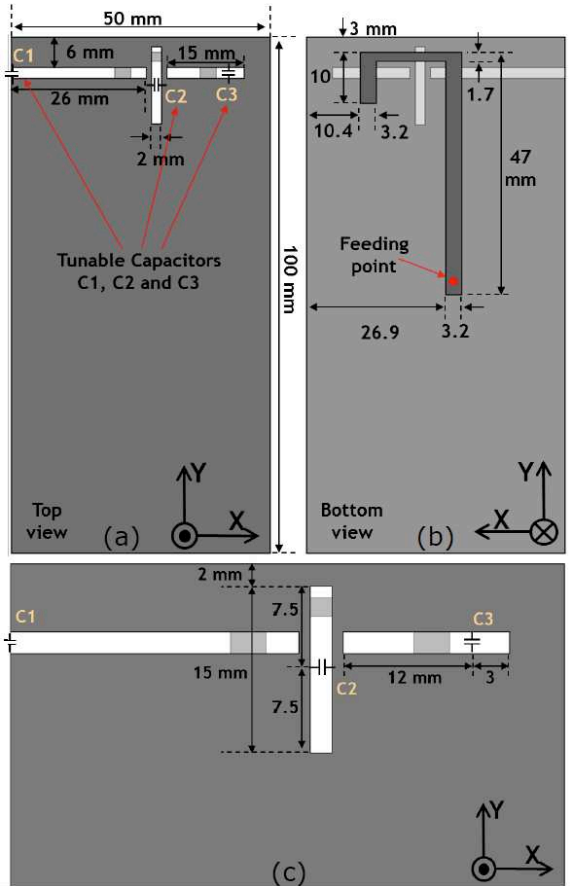

Fig. 2. Tunable, tri-band filtenna geometry: (a) front layer, (b) back layer, (c) tunable capacitor locations.

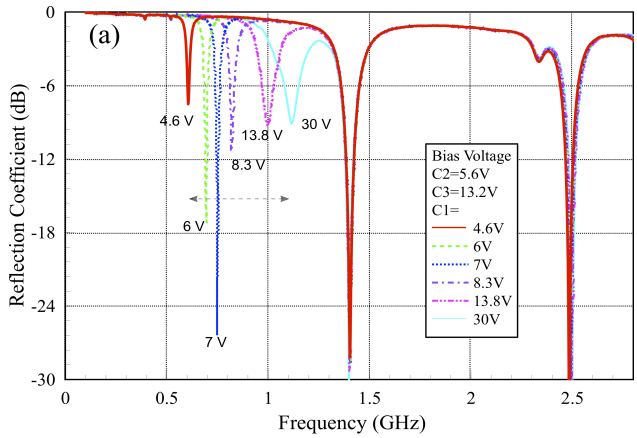

Fig. 3. Measured reflection coefficients (S_{11}) demonstrating the tuning of slot 1 while slots 2 and 3 are fixed.

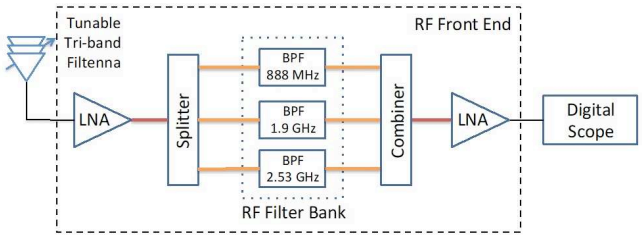

Fig. 4. Schematic block diagram of the concurrent, tri-band RF front-end

A. RF Front-End

The first component of the RF front-end is a tunable tri-band antenna (Fig. 2). It consists of three slots on a ground plane designed to have similar dimensions to a MS PCB (50 x 100 mm). Each slot resonates at a different frequency, with the leftmost slot resonating at the lowest frequency and the rightmost at the highest (Fig. 2 (a)). The slots have been placed to minimize cross-coupling between the elements, but all are fed by the same microstrip line (Fig. 2 (b)). A varactor diode is soldered across each slot, providing a tunable capacitance, which can be used to tune the resonant frequency of each slot independently. This antenna design was presented in [7].

Within the system, the tunable triband antenna acts as the first stage of filtering. By using an antenna with multiple narrow, tunable bands, rather than a broadband antenna, some rejection of out-of-band interference is achieved. This is particularly important for this system, where direct RF digitization is used, as strong out-of-band interferers can lead to receiver desensitization and loss of system performance. However, it should be noted that the bandwidths of each antenna resonance varies with tuning from 9 MHz to 140 MHz [7], so the antenna should not be relied on for strong rejection of immediately adjacent bands. The S_{11} of the antenna, showing fixed bias for the upper two bands while tuning is performed over the lower band, is shown in Fig. 3.

The rest of the RF front-end is shown in more detail in Fig. 4. The received signals, filtered by the antenna, pass to a Mini-circuits ZX60-83LN12+ LNA, which produces a typical 21dB gain over a range of 0.5 GHz to 8 GHz. The specified noise figure (NF) is 1.4 dB, and the linearity performance is good with IP3 of +35.2 dBm at 2 GHz. This suggests it is able to amplify the three distinct RF signals required, which may have large dynamic ranges associated with them, without adding notable distortion.

Both the RF power splitter and combiner are Mini-circuits ZN4PD1-63HP-S+ devices, which are 4 – 1 splitter/combiners. These have been repurposed for 3-band performance by terminating the unused ports with 50 Ω loads to minimise reflections. They have a nominal operating bandwidth of 250 MHz to 6 GHz with insertion loss of 1.0 dB, suggesting little loss of performance from the splitting and recombining of the signals across the sub-6 GHz operating region. Further, they are capable of handling up to 2W RF power, which is well above the expected dynamic range. Isolation between ports is high, at 24 dB, and there is a small imbalance, of 0.2 dB in

magnitude and 2° in phase. As such, the splitter and combiner do not distort the RF signals noticeably.

After the splitter, the identical versions of the RF signal are fed into three distinct SAW filters, which each have a bandpass characteristic. These are TAI-SAW Technology Co. Ltd devices with part numbers TA1889A, TA2018A, and TA1683A; and have fixed centre frequencies of 888.75 MHz, 1.90 GHz and 2.53 GHz, respectively. Their nominal insertion losses are 1.4 dB for the lower filters and 1.3 dB for the higher ones, and have bandwidths of 17.5 MHz, 40 MHz and 20 MHz, respectively. Finally, the stop-band rejection losses are greater than 40 dB in each case. These SAW filters provide the close filtering required for minimising the effects of out-of-band interference on the receiver. Note that, at present, they operate at fixed frequencies, so are not tunable.

However, due to each desired RF signal only being passed by one of the three filters, in addition to the insertion loss of the splitter, combiner and filters, the total received power of each band of interest is reduced by approximately 12.3 dB compared with using a single RF chain for each band. As such, a second amplifier is used, in particular another Mini-circuits ZX60-83LN12+ LNA in order to minimise the receiver NF. Placing this directly before the direct digitisation of the wideband RF signal ensures that the RF front-end rather than the ADC process dominates noise effects in the receiver. The total RF front-end gain was measured at over 25 dB per band.

B. Digital Back-End

The ADC was realized using a Teledyne LeCroy WAVERUNNER 8404M-MS oscilloscope, with an input bandwidth of 4 GHz, sampling rates controllable up to 40 GSample/s and resolution of 8 bits. For the purposes of this paper, experiments were carried out using a fixed sampling rate of 10 GSample/s, providing an oversampling rate of 3.95 for the highest band of interest, 2.53 GHz, which is approximately twice the Nyquist rate. The Texas Instruments ADC12DJ5200RF meets this sampling requirement albeit with a relatively high power consumption of 4W. However, low power, fast sampling ADC techniques for 5G and beyond is an active research area [8]. The oscilloscope's input voltage range was usually set to 40 mV, the lowest value available for the 4 GHz input bandwidth circuitry, so minimizing the quantization error of the digital system as far as possible. Where the received RF signal exceeded this range, such as when high power interfering signals were examined, the input voltage range was increased to capture the whole dynamic range of the waveform.

The digitized RF signal was then transferred over a 100 Mbit/s Ethernet cable to a National Instruments (NI) PXIe-8135 controller. Using the controller's LabVIEW Communications Suite. DDC is performed on each band through digital numerically controlled oscillators (NCOs), recovering digital baseband data. Subsequent processing using LabVIEW's LTE Application Framework (LTE-AF) operating on the PXIe Controller's FPGAs obtains the digital constellation on the LTE Physical Downlink Shared Channel (PDSCH), and an EVM measurement is made. The constellation is demodulated to obtain transport blocks, on which a cyclic redundancy check (CRC) is performed to determine if a transmit error has occurred. This is used to calculate the BLER of the transmission.

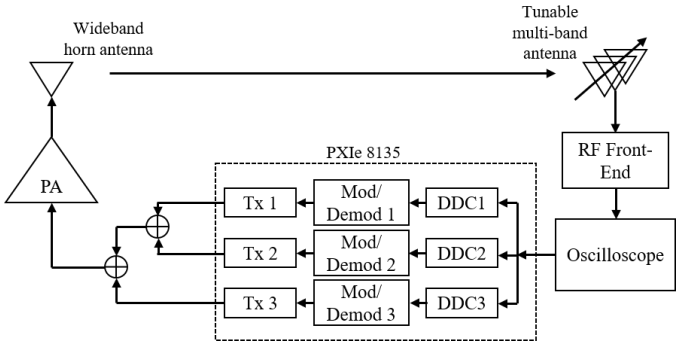

Fig. 5. Schematic block diagram of the tunable, concurrent, tri-band, software defined radio receiver hardware-in-the-loop testbed.

III. TESTBED CONFIGURATION

A hardware-in-the-loop testbed was developed to measure the performance of this single RF chain, concurrent tri-band receiver (Fig. 5). For demonstration of performance with modern complex signaling techniques, LTE waveforms carrying 16-QAM modulation on their physical layer are used as the signal under test. This is an advance on previous work in this area, which has demonstrated QPSK modulation [9]. Three 16-QAM LTE signals were transmitted independently from the PXIe controller: one at a carrier frequency of 888 MHz using an NI-5793 FlexRIO RF Adapter Module controlled by LabVIEW's LTE-AF; and two at 1.92 GHz and 2.53 GHz, respectively, using two NI-5791 FlexRIO RF Adapter Modules controlled by separate LabVIEW TRANSMITTERS. Note that the transmit power, modulation and input data for each of these signals is completely independent, and none of these three signals was synchronized with the others, thereby emulating a heterogeneous network use case.

The signals were combined using two Mini-circuit ZAPD-2-272-S+ 2-signal combiners, then amplified by a Pasternack PE15A4019 wideband power amplifier (PA), which provides a nominal 36 dB gain over 60 MHz to 6 GHz. This allows the signals to reach high enough received powers to act as strong interferers when required. The signals are carried over coaxial cables into an anechoic chamber, in order to minimize reflections and external interference, and transmitted by a UHALP-9108A wideband horn antenna. The signals are received by the tunable triband antenna, biased at 10.0 V, 9.25 V and 14.0 V to give resonance at each centre frequency of interest, and fed to the rest of the receiver.

This paper is particularly interested in the performance of this receiver when undergoing reception of different signal strengths, in particular the case where one band has a significantly lower received power than the other two bands of interest. This is a special case of the near-far problem, which multi-band single-RF chain receivers must overcome, where strong signals from some bands may desensitize the receiver to a weaker signal in a different band, leading to a loss in system performance. To evaluate this, the BLER and EVM of the 888

MHz band are measured as received power is varied, while the 1.92 GHz and 2.53 GHz bands are held at a (relatively high) received power of -50 dBm. This is chosen due to the 3GPP LTE standard requiring receivers to operate acceptably when interfering signals are 39 dB above the nominal reference sensitivity (REFSEN) of -89 dBm [10]. This will be compared with the performance of the receiver when only the 888 MHz band is present, to demonstrate the resilience of the concurrent, tri-band receiver architecture under extreme conditions.

IV. Measurements

First, in order to establish the operational performance of the single-RF chain receiver, the 888 MHz band was measured when the testbed was transmitting only this band, meaning no interference is introduced by the other bands. The received power was calculated by taking the baseband power at the output of the DDCs, and adjusting for the measured gain of the RF front-end for 888 MHz, which was 31.1 dB. These results are then compared with the performance of the 888 MHz band when the testbed was transmitting all three bands, with the two higher carriers held at -50 dBm received power while the power in the lowest band was varied, as mentioned.

The measured EVM decreases with increased received power for both the single band and concurrent measurement, as expected (Fig. 6). Both are able to reach stable EVMs of 5% at high transmit powers, though reduction below this is limited by quantisation error introduced by the ADC. However, 5% is comfortably below the 12.5% value required by the LTE standard for 16 QAM [11]. This level is passed by the receiver at a received power of approximately -73 dBm under single band conditions, and with only 3 dB degradation when reception is concurrent. Note that no measured EVM values are obtained above 50%, due to synchronization and channel estimation failing at these signal to noise ratios (SNRs).

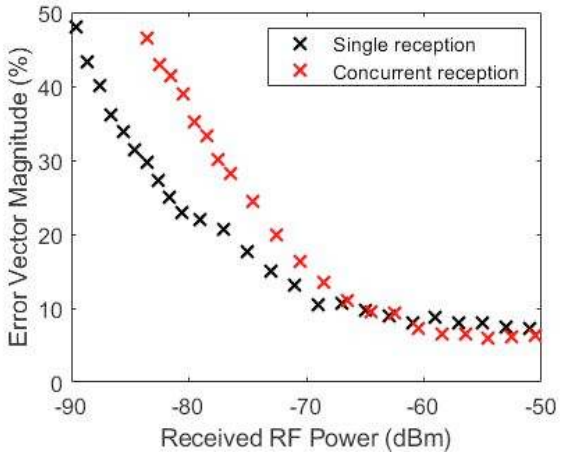

Fig. 6. EVM versus received power for single band and concurrent reception.

The increase in EVM at the same receive power is due to the desensitization of the receiver by the higher bands – in particular, the ADC input range largely consists of the sum of these two signals, with the desired 888 MHz signal superimposed. As such, greater quantisation error is introduced to the band of interest, increasing the EVM. This further explains why the difference reduces as the received power of the desired band is increased, as a greater portion of the RF signal is due to the desired band, thereby reducing the quantisation error.

Figure 7 plots BLER versus received RF power for both single band and concurrent band reception. Both single and concurrent band measurements successfully reduced their BLER below 5%, which is the target error level denoting acceptable performance in the 3GPP LTE standard. In the single band case, this is reached at a received RF power of -84 dBm, which is 5 dB greater than the measured reference sensitivity for QPSK in this band, as described in the LTE standard [10]. Some of this reduction in performance is due to the higher modulation order used here, whereas the excess is due to the increase in noise power attributable to the wideband ADC input. In the measurement campaign, the BLER performance exhibited an error floor of approximately 1%, which is attributed to spurious losses of block synchronization and is currently under investigation.

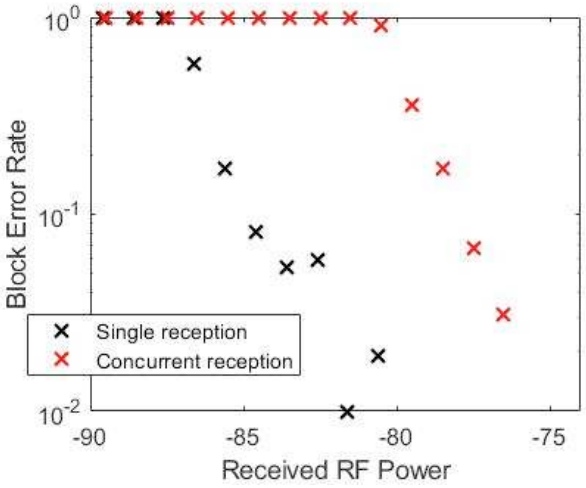

Fig. 7. BLER versus received power for single band and concurrent reception.

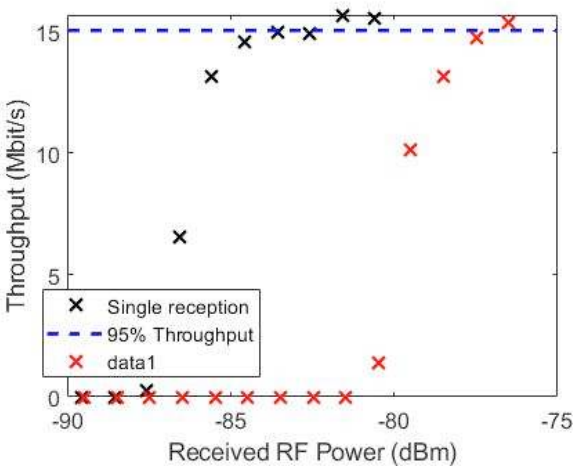

Fig. 8. Throughput versus received power for single band and concurrent reception.

When concurrent reception is considered, the 5% BLER is reached at -78 dBm, with 6 dB degradation compared to the single band case. This is due to the receiver desensitization discussed earlier. Note that it is larger than the degradation in reaching the desired EVM for 16-QAM, due to the in-band received power required to achieve the 5% BLER performance being 10 dB less than that required for the EVM measure, in large part because of the forward error correction coding scheme used in LTE. The quantisation error is higher when the power differences between bands are higher, meaning the degradation in crossing these metrics due to desensitization is greater for the BLER performance than the EVM performance. Importantly, the BLER rather than the EVM level determines the system throughput performance as discussed below.

The throughput for both scenarios is presented in Fig. 8. This has been calculated using the BLER and the known maximum throughput for 16-QAM LTE with 20 MHz bandwidth and coding rate 1/3, which is 15.84 Mbit/s. As with the BLER performance, the 95% throughput threshold is reached by the receiver with both single band and concurrent reception, with degradation of 6dB for the latter. This demonstrates that the single-RF chain receiver is able to concurrently receive three separate bands, with a penalty of 6dB when one received signal is significantly lower than the other two. Future work will complete the system performance evaluation for all three bands.

V. Conclusions

A single-RF chain receiver capable of simultaneously receiving and processing up to three different radio bands has been presented, implemented in a testbed, and its performance has been measured. The compact RF front-end, consisting of a tunable tri-band antenna, wideband LNA and narrowband SAW filters, reduces interference while minimizing added noise and proved to be extremely stable. A 10 GSample/s ADC directly digitizes the RF signal, allowing separate DDCs to provide filtered digital baseband signals to separate SDRs. As such the receiver is flexible in both frequency and across standards, enabling compact and energy efficient aggregation of data streams in heterogeneous networks. Research is underway to extend this work from sub-6 GHz to mm-Wave frequencies (EPSRC grant number EP/S008101/1).

Acknowledgment

The work reported was financially supported by the UK's "Engineering and Physical Sciences Research Council" (EPSRC) on grant number EP/M013723/1.

References

[1] W. Saad, M. Bennis and M. Chen, "A Vision of 6G Wireless Systems: Applications, Trends, Technologies, and Open Research Problems," in *IEEE Network (Early Access)*.

[2] T. S. Rappaport *et al*., "Wireless Communications and Applications Above 100 GHz: Opportunities and Challenges for 6G and Beyond," in *IEEE Access*, vol. 7, pp. 78729-78757, 2019.

[3] F. Hu, B. Chen and K. Zhu, "Full Spectrum Sharing in Cognitive Radio Networks Toward 5G: A Survey," in *IEEE Access*, vol. 6, pp. 15754-15776, 2018.

[4] 3GPP, "NR Carrier Aggregation for intra-band (m Down Link (DL) / 1 Up Link (UL) bands) and inter-band (n Down Link (DL) / 1 Up Link (UL) bands)", Release 15, TR 37.865-01-01, 2017.

[5] H. Ishikawa, "Software defined radio technology for highly reliable wireless communications," in *Wireless Personal Communications*, vol. 64, no. 3, pp. 461-472, June 2012.

[6] K.J. Mitola, "The software radio architecture," in *IEEE Communications magazine*, vol. 33, no. 5, pp. 26–38, 1995.

[7] Q. Bai, R. Singh, K. L. Ford, T. O'Farrell and R. J. Langley, "An independently tunable tri-band antenna design for concurrent multiband single chain radio receivers," in *IEEE Transactions on Antennas and Propagation*, vol. 65, no. 12, pp. 6290-6297, Dec. 2017.

[8] J. Liu, Z. Luo and X. Xiong, "Low-Resolution ADCs for Wireless Communication: A Comprehensive Survey," in *IEEE Access*, vol. 7, pp. 91291-91324, 2019.

[9] M. R. Anbiyaei, S. M. Asif, T. O'Farrell, K. L. Ford and R. J. Langley, "Tunable, concurrent, tri-band single chain radio receiver for 5G New Radio," in *42nd Meeting of World Wireless Forum (WWRF)*, Tokyo, Japan, May 2019.

[10] Evolved Universal Terrestrial Radio Access, "LTE; Evolved Universal Terrestrial Radio Access (E-UTRA); User Equipment (UE) conformance specification; Radio transmission and reception; Part 1: Conformance testing (3GPP TS 36.521-1 version 12.3.0 Release 12)," 2014.

[11] Evolved Universal Terrestrial Radio Access, "LTE; Evolved Universal Terrestrial Radio Access (E-UTRA); User Equipment (UE) radio transmission and reception (3GPP TS 36.101 version 10.2.1 Release 10)," 2011.